



*Iranian Society of  
Acoustics and Vibration*

# The 13<sup>th</sup> ISAV2023 International Conference on Acoustics and Vibration

20, 21 Dec 2023      Tehran - Iran

## Optimizing Vortex Shedder for Vortex Flow Meter Using Deep Learning

Mostafa Khanalipour<sup>a\*</sup>, Hossein Mohammadi<sup>b</sup>

<sup>a</sup> *Master student, School of Mechanical Engineering, Shiraz University, Molla Sadra St., Shiraz, Iran, 71936-16548*

<sup>b</sup> *Associate professor, School of Mechanical Engineering, Shiraz University, Molla Sadra St., Shiraz, Iran, 71936-16548*

\* *Corresponding author e-mail: [mostafakhanalipoor@gmail.com](mailto:mostafakhanalipoor@gmail.com)*

### Abstract

The vortex flow meter is widely employed within the industry as one of the primary flow measurement devices. It operates on the principle of vortex shedding. One of the primary challenges in the design and development of this flow meter lies in the design of the vortex shedder. The vortex shedder must generate strong vortices to enable accurate sensor detection. Given the necessity for extensive experiments and computational fluid dynamics (CFD) analysis in the design of new bluff bodies, this process is both time-consuming and expensive. To address this issue, we employ machine learning (ML) models for the development of new vortex flow meters. We have developed two ML models that aid in the design of new bluff bodies based on deep learning (DL) architectures. These models were trained on both a fully connected deep neural network (DNN) and a convolutional neural network (CNN) architecture, yielding comparable performance. To facilitate model training, we compiled a comprehensive dataset from existing literature, paying particular attention to the symmetrical profiles of bluff bodies. The dataset exclusively contains point coordinates (X, Y) from the right half of the bluff body's cross-section, this consideration leads to more smooth generated shape. The first model was designed to generate new bluff body geometries based on input parameters such as Reynolds number, Strouhal number, and other geometric parameters. The second model focused on predicting the linearity of Strouhal numbers for these generated shapes. The models demonstrated an error rate of approximately 2.80% in the validation phase. These results indicate the potential utility of this approach in the initial phases of bluff body design.

**Keywords:** Vortex flow meter; Vortex shedder; Deep learning; Shape Optimization.

---

## 1. Introduction

Vortex flowmeters stand as one of the most extensively employed flow measurement devices in various industrial applications. Operating on the principle of vortex shedding, these meters harness

the disruptive influence of a bluff body placed within a flowing fluid, giving rise to a rhythmic shedding of vortices downstream of the body (Fig. 1). The frequency at which these vortices are shed correlates directly with the flow velocity. Crucial to the efficacy of vortex flowmeters are the production of Strong vortices by the vortex shedder.

One of the principal challenges encountered in the development of vortex flowmeters centers on the design of this essential vortex shedder component. Complicating matters further, many established bluff body shapes are subject to copyright restrictions, necessitating the exploration of novel bluff body designs for the advancement of vortex flow measurement technology. The design of an effective vortex shedder is a complex process that requires a deep understanding of fluid dynamics, extensive experimentation, and often computational fluid dynamics (CFD) analysis. These endeavors, while indispensable, can be very time-consuming and financially burdensome.

Recent years have witnessed the emergence of Machine Learning (ML) as an influential presence in engineering disciplines. Within the domain of fluid dynamics, ML has demonstrated its capabilities in the study of turbulence [1], [2], [3], flow control [4],[5], flow simulation using deep learning models [6], prediction of vortex-induced vibrations [7], [8], and the accurate prediction of fluid field characteristics [9]. Notably, the geometric configuration of the bluff body profoundly influences the performance of vortex flow meters. An ideal bluff body should incite a strong flow fluctuations over a broad range of Reynolds numbers [10].

In pursuit of optimal shapes, previous research has made substantial efforts. Igarashi [11], for instance, scrutinized the vortex-shedding characteristics of six bluff bodies with diverse cross-sectional shapes, pinpointing the superiority of a circular cylinder with a slit in enhancing vortex strength. Bently and Nichols [12] proposed a dual bluff body arrangements to enhance the quality of vortex-shedding signals. Venugopal et al. [10] conducted experimental investigations into various bluff bodies with distinct forebody and afterbody shapes, ultimately endorsing the trapezoidal bluff body as the most suitable configuration, grounded in its constancy within the  $St-Re$  relationship. Miao et al. [13] took an innovative approach, employing a trapezoidal T-shaped body as a vortex shedder, showcasing improvements in vortex shedding stabilization and the linearity of the  $St-Re$  relationship, credited to the optimal length of the extended plate. However, many of these optimal shapes, while theoretically compelling, are geometrically intricate and face practical constraints on manufacturability, economics, and reliability.

In a notable stride towards overcoming these challenges, D. Thummar [14] employed machine learning techniques to design innovative bluff bodies for vortex flow meters, offering a potential solution to this longstanding conundrum. Building upon this foundation, our work endeavors to leverage deep learning methodologies to expedite the bluff body design process.

This article is structured as follows: we commence with a detailed discussion of the steps involved in data collection within the Deep Learning section, followed by an exploration of the fundamental principles underpinning deep learning architectures. Subsequently, we delve into the specifics of training models and validate the results through the utilization of CFD simulations.

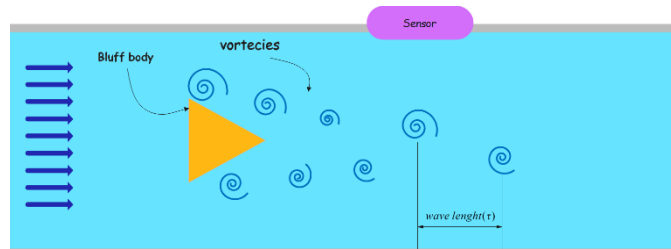


Figure 1: Vortex shedding of a bluff body.

## 2. Deep Learning Approach

One critical facet of developing a supervised machine learning algorithm is the quality of the data it relies upon. In this section, we will delve into the intricate process of data gathering, followed by an exploration of the fundamental concepts within Artificial Neural Networks (ANNs). Specifically, we will elucidate the architectures of Deep Neural Networks (DNNs) and Convolutional Neural Networks (CNNs) for a comprehensive understanding.

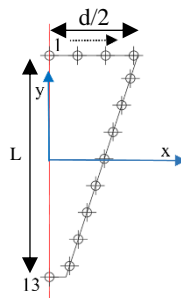
### 2.1 Data Collection

The quality of collected data is very critical in developing DL models. Hence, we tried to collect a robust dataset for this task. bluff bodies with various shapes have been designed and evaluated in the literature. The dataset used in this study is gathered from data that has been recorded in the literature for years.

Influential parameters like  $Re$ ,  $St$ , blockage ratio, Aspect ratio, and shape of the bluff body are selected as features of the dataset. Positions on the bluff body cross-section premier represent bluff body shape. To Study the effect of the number of shape data on DL models we select two sets of data. The first dataset (dataset 1) has 13 (X, Y) positions in the bluff body cross-section and the second (dataset 2) has 41. Other features are the same in both datasets.

The bluff body shape data was obtained by discretizing the right half of the bluff body shape in CAD software and the geometric center of shape was selected as the origin as shown in Fig. 2. Blockage Ratio ( $d/D$ ) gives information about pipe diameter ( $D$ ) compared to bluff body size. The aspect ratio is used to inform the size of the slit in the bluff body ( $s/d$ ) and the length of the bluff body ( $l/d$ ).  $Re$  and  $St$  are the features that give information about fluid flow characteristics. To obtain fluid flow characteristics ( $Re$ ,  $St$ ) from plots in literature we used an image digitization software.

Information about bluff body features is in Table 1. With this set of features, we gathered datasets 1 and dataset 2 with 31 and 87 features respectively. Both datasets have 285 data points. Each dataset contains all the needed features to train both models. One can split data, column-wise, in input and output for both models.



**Figure 2:** Detail on bluff body discretization.

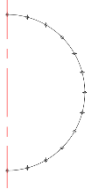

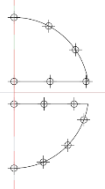

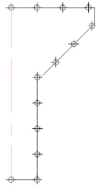
Model 1 is trained to generate new bluff body geometries. The inputs of this model are  $Re$ ,  $St$ , Blockage ratio, and aspect ratio. In the output, it gives the bluff body geometry estimate for a set of inputs. It contains 13 points (or 41 for models trained on dataset 2) which is the right half of the predicted bluff body shape. Due to symmetry, these points can easily be used to draw the left half.

Model 2 input is bluff body predicted shape,  $Re$ , blockage ratio, and aspect ratio and estimate the Strouhal number for the given shape and the parameters used to generate the shape. This model can also be used to check linearity in  $St$  for any range of Reynolds. To create an accurate ML model, all features should be small with low variance. Reynolds number has a high range in the datasets and can lead to low accuracy in models. Hence, the Reynolds number was normalized after creating datasets. To normalize data one can use Eq. (1).

$$x' = \frac{x - \mu}{\sigma} \quad (1)$$

Where  $\mathbf{x}'$  is the normalized feature Vector,  $\mathbf{x}$  is the input vector,  $\mu$  is the feature mean and the  $\sigma$  is the standard deviation input. To train both models, datasets were divided into sets of 80% and 20% for training and test datasets respectively.

**Table 1:** Details on data resources and dataset.

Bluff body shape					
	Circle	Triangle	Circle with slit	Trapezoidal	T-Shaped
Author	Venugopal et al.[14]	Zhang et al.[15]	Peng et al.[16]	Venugopal et al.[14],[17]	Miau et al.[13]
Re range	500-400000	100000-300000	2000-15000	500-150000	2000-20000
St range	0.2-0.45	0.2-0.5	0.2-0.27	0.1-0.38	0.065-0.222
Geometrical parameters	$d/D = 0.14-0.25$ ,	$\theta = 60^\circ$ , $d/D = 0.2-0.38$	$s/d=0-0.3$ , $d/D=0.1$	$l/d=1.25$ , $d/D=0.14-0.28$	$d=32$ mm, $a=3$ mm, $b=10$ mm, $l/d=0-3.13$ , $d/D=0.2703$
No. data points	80	24	47	99	35

## 2.2 Artificial neural network details

Artificial Neural Networks (ANNs) and Convolutional Neural Networks (CNNs) are powerful machine learning tools. These networks are capable of learning complex patterns and relationships in data, making them particularly valuable for nonlinear regression tasks. In a DNN we have an input layer, some hidden layers, and an output layer as shown in Fig. 3. A hidden layer is connected to its previous layer with a set of weights. The mathematical equation for hidden layers is in Eq. (2) [18].

$$\mathbf{h} = g(\mathbf{W}^T \mathbf{x} + b) \quad (2)$$

Where  $\mathbf{x}$  is the input vector,  $\mathbf{W}$  is the weight matrix,  $b$  is the bias,  $\mathbf{h}$  is the output vector, and  $g$  is the activation function. To introduce nonlinearity in a neural network we should use a nonlinear activation function. A common activation function for hidden layers is the Rectified Linear Unit (ReLU). ReLU is defined as  $g(z) = \max(0, z)$ . We used the ReLU activation function for training all models. In all models, Mean square error (MSE) was used as the loss function. It is shown in Eq. (3).

$$MSE \text{ loss} = \mathbb{E} \left( \|\mathbf{y} - f(\mathbf{x})\|^2 \right) \quad (3)$$

Where  $\mathbf{x}$  is the input,  $f(\mathbf{x})$  the is neural network prediction, and  $\mathbf{y}$  is the input true value.

A CNN consists of several convolution layers after the input layer. The output of the convolution layers then goes to the hidden layers. The last layer is the output. A schematic of the CNN is in Fig. 4. When we use a kernel for the convolution layer, we need to know the length of the output vector after applying this kernel. We can calculate it by using eq. (4).

$$L_{out} = \text{floor} \left[ \frac{L_{in} + 2 \text{ padding} - \text{dilation} (\text{Kernel size} - 1) - 1}{\text{stride}} + 1 \right] \quad (4)$$

Where  $L_{in}$  is the input vectors length. Padding, stride, and dilation are the features of the kernel of the convolution layer.

Both models were trained on a DNN and a CNN to compare architectures. For training models, Adam optimization algorithm was employed that is a gradient-based optimization algorithm.

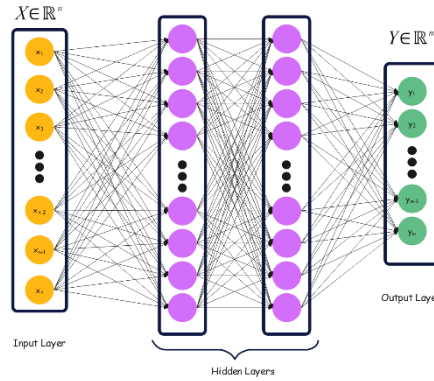


Figure 3: Deep neural network architecture.

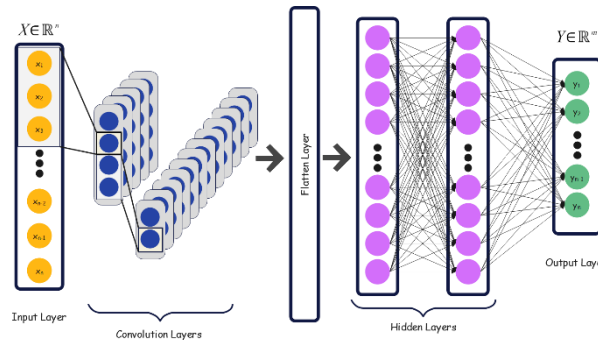


Figure 4: Convolutional neural network architecture.

### 2.3 Artificial neural network training process

For building and training neural networks we used the PyTorch library. Dropout regularization has been used for models to overcome the overfitting issue. Some models' performance was better with dropout. K-fold cross-validation and trial-and-error approach have been employed to find the best hyperparameters for each model. ReLU activation function used to train all models. The Mean square Error has been set as the loss function. Adams optimization algorithm has been used to optimize models' weight.

Model 1 with dataset 2 has an input layer, four hidden layers, and an output layer. The input layer accepts vectors of length five, which are  $L/d$ ,  $d/D$ ,  $Re$ ,  $St$ ,  $s/d$  in order. The number of neurons in the hidden layer one through five is 45, 125, 450, and 180 in order. A dropout layer with probability of 15% has been used for all hidden layers. The output layer size is 82, which are the points in the generated shape. The first 41 numbers are X positions, and the last 41 numbers are Y positions.

Model 2-CNN with dataset 2 has three convolution layers, eight hidden layers, and an output layer. All convolution layers use the kernel size of 5, padding of 2, and stride equal to 2. The number of Output channels for layers one to three are 15, 45, and 80. The number of neurons in hidden layers are 950, 1300, 1800, 1000, 400, 230, and 100 in order. Dropout layer with the probability of 30% has been used for all hidden layers. The learning rate for training models is in Table 2.

**Table 2:**The learning rate of optimizer for trained models.

	Model 1 Dataset 1	Model 1 Dataset 2	Model 1-CNN Dataset 1	Model 1-CNN Dataset 2	Model 2 Dataset 1	Model 2 Dataset 2	Model 2-CNN Dataset 1	Model 2-CNN Dataset 2
<b>Learning rate</b>	0.001	0.01	0.001	0.01	0.01	0.001	0.002	0.001

### 3. Results and discussions

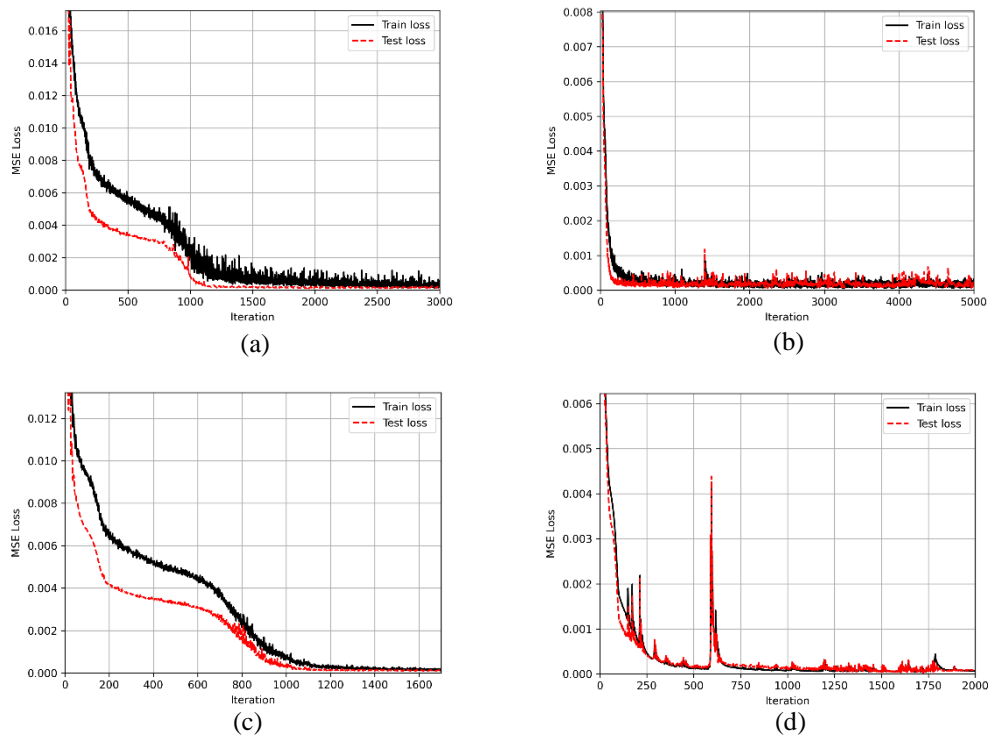
After creating dataset, we will train DL models on these datasets and use these models to get a vortex shedder and evaluate its optimality. Then we will use simulation to validate models output.

#### 3.1 Training Deep Learning models

Models were created and optimized with the PyTorch library. The value of the loss function for both the test and train datasets are in Table 3. The loss values shows that all models are converged and overfit was not occur. The value of the loss function per iteration for training Model 1 and Model 2 are shown in Fig. 5 and Fig. 6 respectively.

**Table 3:** Loss value in the last iteration of training models.

	Model 1 Dataset 1	Model 1 Dataset 2	Model 1-CNN Dataset 1	Model 1-CNN Dataset 2	Model 2 Dataset 1	Model 2 Dataset 2	Model 2-CNN Dataset 1	Model 2-CNN Dataset 2
<b>Train loss</b>	2.06e-4	3.11e-4	1.09e-4	6.63e-5	1.30e-4	9.15e-5	9.63e-5	1.50e-4
<b>Test loss</b>	1.72e-4	1.17e-4	1.00e-4	7.17e-5	1.68e-4	1.29e-4	1.29e-4	1.78e-4



**Figure 5:** MSE Loss Vs iteration for a) Model 1- dataset 1, b) Model 1- dataset 2, c) Model 1-CNN dataset 1, d) Model 1-CNN dataset 2.

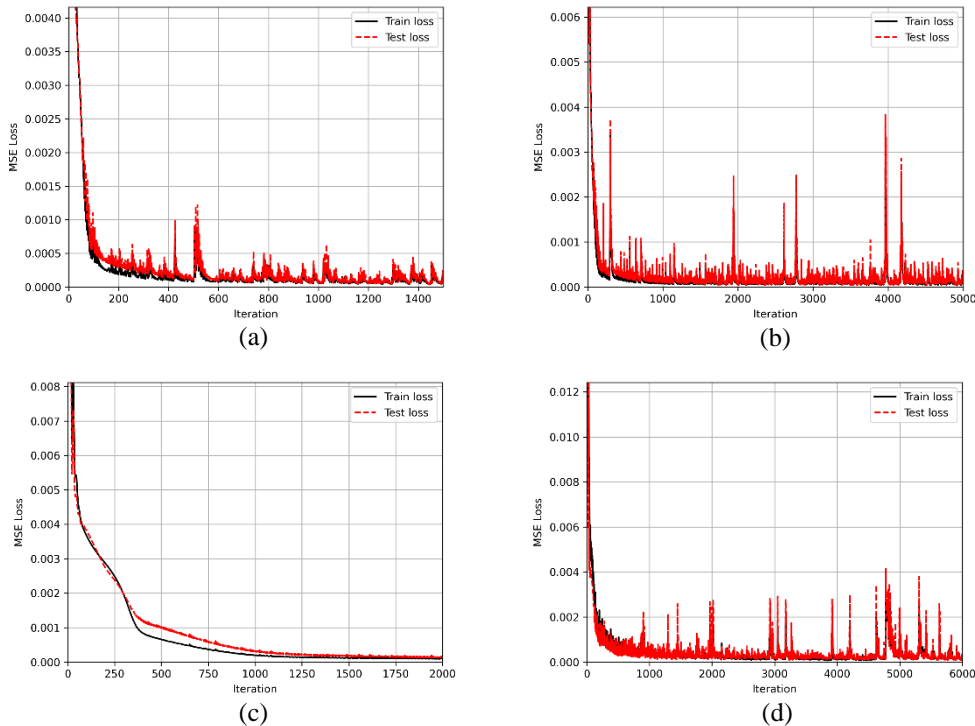
#### 3.2 Deep Learning models robustness

We collected two datasets to see how sensitive are the models with several geometric points. To check the robustness, we give Model 1 in all 4 cases the same input to generate a bluff body shape. Generated Bluff body shapes are depicted in Fig. 7. All shapes are very similar that shows the data collection approach was suitable. Considering symmetry in the data collection phase helped to

achieve this robustness. It's expected that the models trained with more data generate more accurate shapes.

### 3.3 Vortex shedder optimization for linearity

An optimized bluff body will have a low standard deviation in a large range of Reynolds. When we use a Machine learning model to obtain these shapes, another consideration is how the predicted shape is interpretable and one can draw the shape without any guess about it. We used the first Model to generate an optimized bluff body shape with different Reynolds and different shape features. Since Model 1 trained in dataset 2 generated shapes seem to be more accurate, we used this model to generate new shapes. The shape depicted in Fig. 7.c was selected as an optimal new shape. After that Model 2 was employed to predict Strouhal number and its linearity on this shape.

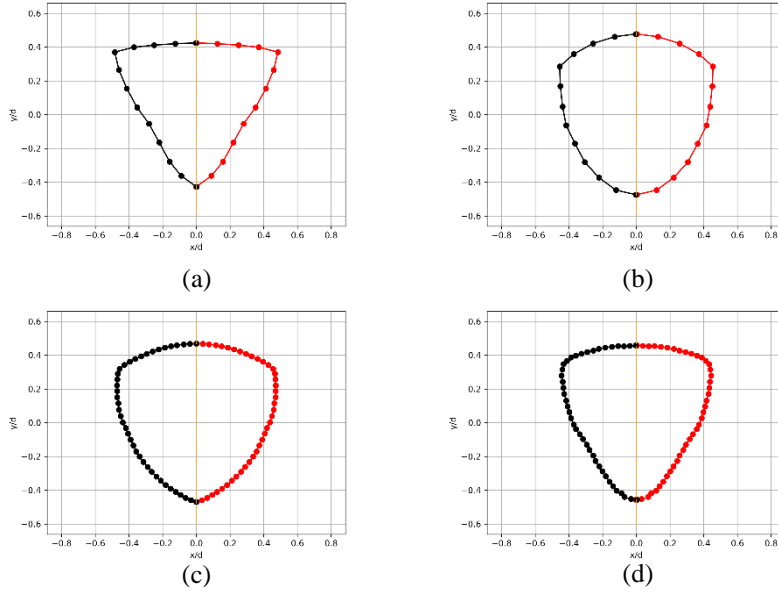


**Figure 6:** MSE Loss Vs. iteration for a) Model 2- dataset 1, b) Model 2- dataset 2, c) Model 2-CNN dataset 1, d) Model 2-CNN dataset 2.

To validate the linearity of the Strouhal number, we used Model 2 to predict  $St$  for two Reynolds numbers. The results are shown in Table 4. Since ML models are not aware of physical laws, we need simulation to verify the models' output. Although simulation doesn't guarantee all future predictions of models it just shows that some models' outputs are valid.

**Table 4:** Strouhal number prediction with Model 2 for the selected shape.

	Model 2 dataset 2	Model 2-CNN dataset 2
<b>Re = 80,000</b>	0.2689	0.2604
<b>Re=100,000</b>	0.2690	0.2612



**Figure 7:** Predicted shape with  $Re=100000$ ,  $St= 0.3$ ,  $l/d=0.2$ ,  $d/D=0.25$ ,  $s/d=0$  as input parameters, with a) Model 1 - dataset1, b) Model 1-CNN dataset 1, c) Model 1 - dataset 2, d) Model 1-CNN dataset 2.

### 3.4 Validation with CFD simulation

To validate ML models, we need CFD simulation on predicted shapes. A CFD simulation has been done for both cases in Table 4. We used FLUENT software for CFD simulation. The simulation has been done for a 2-D, unsteady condition. We considered the bluff body in a 0.1-meter pipe, and the generated bluff body shape scaled to the  $d/D$  ratio. The maximum width of the scaled shape is about 0.028 meters. The flow input is 0.5 meters before the bluff body, and the output is 1.5 meters after that. Water is used as fluid for simulation. The fluid is assumed to be incompressible with constant properties. To modeling turbulence,  $k - \omega(SST)$  turbulence model has been used. The PISO algorithm was used as the Pressure-Velocity Coupling Method. To calculate the velocity of flow we can use the Reynolds number formula in Eq. (5).

$$Re = \frac{v \cdot D \cdot \rho}{\mu} \quad (5)$$

Where  $v$  is the fluid mean velocity,  $D$  is the pipe diameter,  $\rho$  is the fluid density, and  $\mu$  is the fluid dynamic viscosity.

We used a mesh with about 10000 elements for simulation. The simulation time step was the fixed value of 0.001 seconds. With about ten times increase in the number of elements, there was only a 1% change in results. So, the results were converged. Fluctuation in the Lift coefficient was used to obtain the Strouhal number. To calculate  $St$  one can use Eq. (6).

$$St = \frac{f \cdot d}{v} \quad (6)$$

Where  $d$  is the vortex shedder maximum width, and  $f$  is the vortex shedding frequency. The Fast Fourier Transform (FFT) of the lift coefficient signal for both cases are shown in Fig. 8. With these results and eq. (6) one can calculate  $St$  in both conditions. The comparison of DL models predicted  $St$  with the real one is in Table 5. The results show that the trained models' prediction is accurate. The model with CNN Architecture approximates the  $St$  value better than the other model.

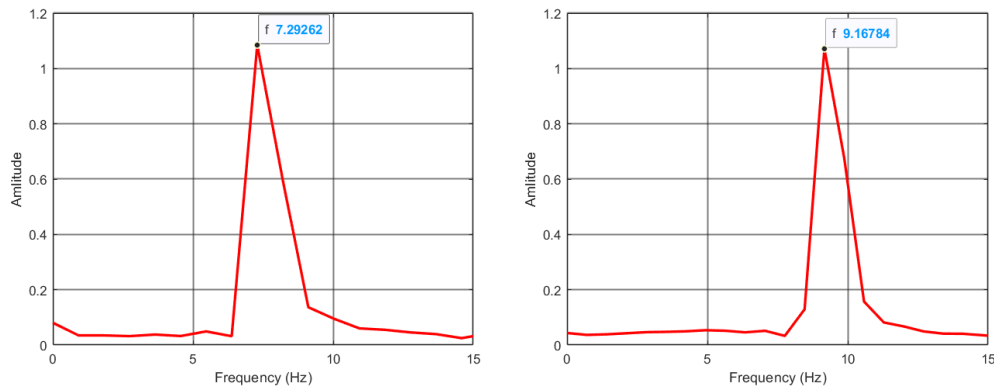


**Table 5:** Comparison of simulation results with ML outputs.

	St-CFD	St-Model 2	Model 2 Error	St-Model 2-CNN	Model 2-CNN Error
Re = 80,000	0.2543	0.2689	5.74%	0.2604	2.40%
Re = 100,000	0.2557	0.2690	5.20%	0.2612	2.15%

### 3.5 Discussion

The Predicted shape in Fig. 7.c is used to validate DL models. To validate models a CFD the simulation was done for the predicted bluff body. The results of the simulation are shown in Table 5. According to simulation results shown in Table 5, these models can accelerate the early phase of vortex shedder design. Implementing them in the design process it can reduce parametric design time. These results suggest that ML-based approaches have the potential to significantly accelerate the design and development of vortex flowmeters. ML models can be used to screen a large number of potential bluff body designs quickly and efficiently. This can help engineers identify promising designs that can then be further evaluated using CFD or experimental methods.



**Figure 8:** Vortex shedding Frequency at: a) Re=80000, b) Re=100000.

## 4. Conclusion

In this work, we implemented a deep learning method to estimate new optimized shapes for vortex shedders. Two DL models were trained for that. The first model predicted a vortex shedder shape based on Re, St, and geometry parameters as the inputs. The second model uses the predicted shape in model 1, Re, and geometry parameters. Its output is the Strouhal number. Model 2 was used to estimate the generated shape optimality. Model 1 trained on dataset 2 generate more smooth shapes. Model 2 trained on dataset 2 predicts Strouhal number of a generated shape more accurately. It was shown that using Convolution layers improves the accuracy of Model 2.

To validate the DL models, a CFD simulation has been done for an optimal generated shape. The results show that DNN and CNN model errors are below 5.8% and 2.4% respectively. So, we can use these models to design new optimal vortex shedders. This can reduce the time for developing new vortex shedders by decreasing the number of simulations for obtaining an optimized shape.

## REFERENCES

1. Duraisamy, K., G. Iaccarino, and H. Xiao, " *Turbulence Modeling in the Age of Data.* " Annual Review of Fluid Mechanics, 2019. **51**(1): p. 357-377.
2. Zhu, L., et al., " *Machine learning methods for turbulence modeling in subsonic flows around airfoils.* " Physics of Fluids, 2019. **31**(1).

3. Brunton, S.L., B.R. Noack, and P. Koumoutsakos, " *Machine Learning for Fluid Mechanics.*" Annual Review of Fluid Mechanics, 2020. **52**(1): p. 477-508.
4. Ayli, E., E. Kocak, and H. Turkoglu, " *Machine Learning Based Developing Flow Control Technique Over Circular Cylinders.*" Journal of Computing and Information Science in Engineering, 2022. **23**(2).
5. Zheng, C., et al., " *Data-efficient deep reinforcement learning with expert demonstration for active flow control.*" Physics of Fluids, 2022. **34**(11).
6. Yang, Y. and Y. Mesri, " *Learning by neural networks under physical constraints for simulation in fluid mechanics.*" Computers & Fluids, 2022. **248**: p. 105632.
7. Bai, X.-D. and W. Zhang, " *Machine learning for vortex induced vibration in turbulent flow.*" Computers & Fluids, 2022. **235**: p. 105266.
8. Wang, Z., J. Zhu, and Z. Zhang, " *Machine learning-based deep data mining and prediction of vortex-induced vibration of circular cylinders.*" Ocean Engineering, 2023. **285**: p. 115313.
9. Sekar, V., et al., " *Fast flow field prediction over airfoils using deep learning approach.*" Physics of Fluids, 2019. **31**(5).
10. Venugopal, A., A. Agrawal, and S.V. Prabhu, " *Influence of blockage and shape of a bluff body on the performance of vortex flowmeter with wall pressure measurement.*" Measurement, 2011. **44**(5): p. 954-964.
11. Igarashi, T., " *Flow Resistance and Strouhal Number of a Vortex Shedder in a Circular Pipe.*" JSME International Journal Series B, 1999. **42**(4): p. 586-595.
12. Bentley, J.P. and A.R. Nichols, " *The mapping of vortex fields around single and dual bluff bodies.*" Flow Measurement and Instrumentation, 1990. **1**(5): p. 278-286.
13. Miao, J.J., et al., " *A T-shaped vortex shedder for a vortex flow-meter.*" Flow Measurement and Instrumentation, 1993. **4**(4): p. 259-267.
14. Venugopal, A., A. Agrawal, and S.V. Prabhu, " *On the linearity, turndown ratio and shape of the bluff body for vortex flowmeter.*" Measurement, 2019. **137**: p. 477-483.
15. Zhang, H., Y. Huang, and Z. Sun, " *A study of mass flow rate measurement based on the vortex shedding principle.*" Flow Measurement and Instrumentation, 2006. **17**(1): p. 29-38.
16. Peng, B.H., et al., " *Performance of vortex shedding from a circular cylinder with a slit normal to the stream.*" Flow Measurement and Instrumentation, 2012. **25**: p. 54-62.
17. Venugopal, A., A. Agrawal, and S.V. Prabhu, " *Vortex dynamics of a trapezoidal bluff body placed inside a circular pipe.*" Journal of Turbulence, 2018. **19**(1): p. 1-24.
18. Heaton, J., " *Ian Goodfellow, Yoshua Bengio, and Aaron Courville: Deep learning.*" Genetic Programming and Evolvable Machines, 2018. **19**(1): p. 305-307.